Characterization of the Giant Transient Dipole Generated by Photoinduced Electron Transfer in a Carotene−Porphyrin−Fullerene Molecular Triad

Sergei N. Smirnov,*,† Paul A. Liddell,‡ Ivan V. Vlassiouk,† Alexey Teslja,§,⊥ Darius Kuciauskas,‡ Charles L. Braun,§ Ana L. Moore,*,‡ Thomas A. Moore,*,‡ and Devens Gust*,‡

Contribution from the Department of Chemistry and Biochemistry, Center for the Study of Early Events in Photosynthesis, Arizona State University, Tempe, Arizona 85287-1604, Department of Chemistry and Biochemistry, New Mexico State University, Las Cruces, New Mexico 88003, and Department of Chemistry, Dartmouth College, Hanover, New Hampshire 03755

Received: March 2, 2003

Excitation of a carotenoid (C) porphyrin (P) fullerene (C_{60}) molecular triad yields the porphyrin first excited singlet state, $C-{}^1P-C_{60}$, which decays via a sequential two-step photoinduced electron-transfer process into a $C^{\bullet+}-P-C_{60}^{\bullet-}$ charge-separated state with a lifetime of 340 ns in 2-methyltetrahydrofuran solution. The transient dc photocurrent method has been used to investigate the dipole moment of the charge-separated state in tetrahydrofuran and 2-methyltetrahydrofuran. The results show formation of a giant dipole with a moment in excess of 150 D, corresponding to separated charges located on the fullerene and carotene moieties of the triad.

Introduction

One approach to mimicry of photosynthetic energy conversion has been the construction of large "supermolecules" consisting of covalently linked chromophores, electron donors, and electron acceptors. Such molecules can demonstrate the intramolecular transfer of singlet and triplet excitation energy and photoinduced electron transfer to generate long-lived, energetic charge-separated states. Many of these artificial reaction centers feature porphyrins as the primary light-absorbing species and as models for the chlorophylls of natural reaction centers.[1−6] These molecules not only serve as mimics of natural solar energy conversion, but also as potential components of molecular-scale optoelectronic devices.[7−20] The charge-separated states produced upon excitation are typically the raison d'être for such artificial reaction centers. Although transient absorption techniques may be used to identify these states and follow their formation and decay with time, these techniques do not yield information about the charge distribution character of the states. The dipole moment of a transient charge-separated state is one of its most basic and important properties, but methods for measuring this quantity are limited.

The transient microwave conductivity technique has been applied to a number of systems producing transient dipoles[21−27] and has permitted the determination of important information that was previously unavailable by other methods. However, that technique has intrinsic limitations in time resolution and a requirement for very low solvent polarity. In addition, an estimate for the rotational time of the transient dipolar species is required in order to determine the dipole moment. More recently, it has been shown that the transient dc photocurrent technique not only yields information on the dipole moments of transient charge-separated species but also is compatible with a wide range of solvent polarities, depends only weakly on molecular rotational times, and has subnanosecond time resolution.[28,29]

One type of artificial photosynthetic reaction center prepared to date consists of a porphyrin (P) bearing a carotenoid polyene (C) and an electron acceptor.[1,3,7,30−36] An example is molecular triad **1**, in which the acceptor is a fullerene (C_{60}) moiety.[37] Transient absorption and emission experiments have shown that in 2-methyltetrahydrofuran (MTHF) solution, excitation of the porphyrin moiety of $C-P-C_{60}$ yields, $C-{}^1P-C_{60}$, which decays with a rate constant of 3.3×10^{11} s^{-1} to give a $C-P^{\bullet+}-C_{60}^{\bullet-}$ charge-separated state with a quantum yield of unity. Light absorbed by the fullerene also leads to formation of $C-P^{\bullet+}-C_{60}^{\bullet-}$ with a yield of essentially 1. Competing with charge recombination to yield the ground state ($k_{CR1} = 2.1 \times 10^9$ s^{-1}), electron transfer from the carotenoid ($k_{CT2} = 1.5 \times 10^{10}$ s^{-1}) to yield a final $C^{\bullet+}-P-C_{60}^{\bullet-}$ charge-separated state is facile. In MTHF this species is formed with a quantum yield of 0.88, based upon light absorbed by the porphyrin chromophore.

Although it is clear from the photochemistry discussed above that the $C^{\bullet+}-P-C_{60}^{\bullet-}$ state in **1** must have a very large dipole moment, its exact magnitude is unknown. Even though it is certain that the positive charge resides on the carotenoid moiety, its highly delocalized and polarizable π-electron system makes prediction of the dipole moment in **1** and other carotenoid-containing artificial reaction centers difficult. For this reason, we used the transient dc photocurrent technique to investigate transient dipoles formed after excitation of **1** in 2-methyltetrahydrofuran and tetrahydrofuran.

Results

Transient Absorption Measurements. As mentioned above, the rate constants and quantum yields for the various photophysical and electron-transfer steps for **1** in MTHF at ambient temperatures have been previously reported.[37] The quantum

* To whom correspondence should be addressed.
† New Mexico State University.
‡ Arizona State University.
§ Dartmouth College.
⊥ Currently at Johns Hopkins University.

10.1021/jp034532o CCC: $25.00
Published on Web 08/20/2003

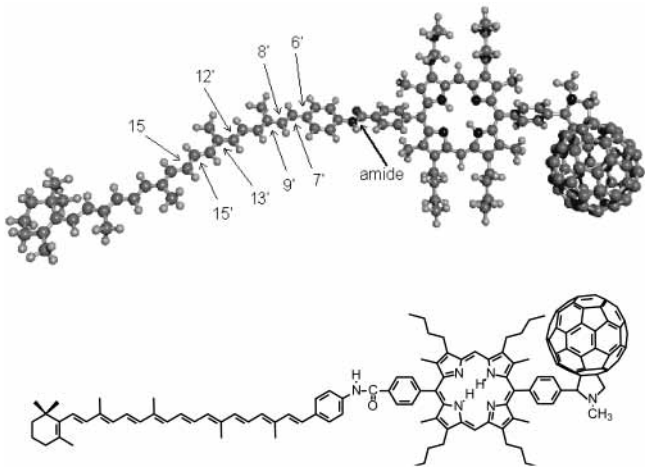

Figure 1. Structure and the lowest-energy conformation for triad **1** as calculated using MM+ molecular mechanics methods. The double bonds in the carotenoid conjugated backbone and the amide partial double bond are all trans. There are several other conformations of essentially equal energy and with similar interatomic distances that can be generated by 180° rotations about the 6′−7′ bond or single bonds in the amide linkage.

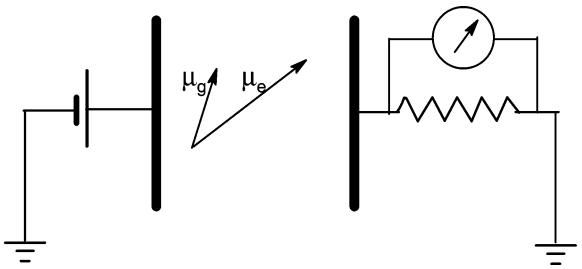

Figure 2. Schematic diagram for the circuit used to measure transient dc photocurrents. The dipole cell comprises two parallel stainless steel electrodes separated by a small gap (to ensure reproducibility, measurements were done with 1.2 and 0.7 mm gaps). The laser irradiation penetrates through a quartz window and between the electrodes to excite a C−P−C_{60} triad solution circulating through the gap. The cartoon illustrates that the ground-state dipole moment, μ_g, is less oriented by the external electric field than the larger excited-state dipole moment, μ_e.

yield of the final $C^{\bullet+}-P-C_{60}^{\bullet-}$ state in tetrahydrofuran (THF) at ambient temperatures has now been determined as well. Solutions ($\sim 1 \times 10^{-5}$ M) of **1** in THF and MTHF were made up with identical absorbance and excited with ~5 ns laser pulses at 575, 590, and 620 nm, where essentially all of the light is absorbed by the porphyrin moiety. The transient absorbance of the carotenoid radical cation in $C^{\bullet+}-P-C_{60}^{\bullet-}$ was monitored near its maximum at 950 nm, and the maximum amplitudes were determined for the two solvents. On the basis of the quantum yield Φ_{cs} (MTHF) = 0.88 for **1** in MTHF mentioned above, a yield of Φ_{cs} (THF) = 0.59 for $C^{\bullet+}-P-C_{60}^{\bullet-}$ in THF was determined.

Molecular Modeling. Interpretation of dipole moment data in terms of molecular structure requires knowledge of molecular structure and conformations. Molecular modeling using the MM+ molecular mechanics approach (HyperChem[38]) yielded the lowest-energy ground-state conformation of **1** shown in Figure 1. This linear extended conformation for the molecule is consistent with previous calculations and NMR determinations of molecular structure for related carotenoporphyrins.[39−41]

Transient DC Photocurrent Measurements. Figure 2 shows a schematic representation of the experimental setup.[29] The sample of triad **1** in solution is excited between two parallel stainless steel electrodes separated by a distance *d* (1.2 and 0.7 mm were used) and confined by two quartz windows. When the sample is excited with a 20 ps laser pulse, photoinduced charge separation generates $C^{\bullet+}-P-C_{60}^{\bullet-}$ as described above. The formation time for that charge-separated state (59 ps in MTHF) is much shorter than the time response of the apparatus (ca. 0.5 ns), allowing us to treat its formation as instantaneous. The final charge-separated state has a different, much larger dipole moment than the ground state. The applied voltage V_0 (500 V) causes the newly formed giant dipoles to reorient with a rotation time, τ_r, causing a change in the angular distribution of dipole moments with respect to the applied electric field. This results in a displacement current measured across a load resistor *R* and digitized on the TDS 684A oscilloscope as a function of time *t*.

The photoinduced voltage, v, associated with the displacement current is described[29] by eq 1

$$v + \tau_{RC}\frac{dv}{dt} = RS\frac{dP}{dt} \tag{1}$$

where τ_{RC} is the *RC* time constant of the circuit with *C* being the cell capacitance and *S* the area of the electrodes. In eq 1 the electric polarization due to solutes, *P*

$$P = n_{cs}\langle\mu_{eff}\rangle \tag{2}$$

evolves due to two factors: the change of the dipole concentration, n_{cs}, recombining with time constant τ_{CR}

$$\frac{dn_{cs}}{dt} = -n_{cs}/\tau_{CR} \tag{3}$$

and the reorientation of the dipoles. The latter is hidden in the average (over all solute dipoles) projection of the dipole moment $\langle\mu_{eff}\rangle$, which is a function of time and the initial distribution. When excitation is symmetric (or made at the magic angle) $\langle\mu_{eff}\rangle$ can be calculated from eq 4[29]

$$\frac{d\langle\mu_{eff}\rangle}{dt} = \left(-\langle\mu_{eff}\rangle + \frac{\langle\mu_{eff}E\rangle}{k_BT}n_{cs}\right)/\tau_r - \langle\mu_{eff}\rangle/\tau_{CR} \tag{4}$$

Here k_B is Boltzmann's constant, *T* is the absolute temperature, and we label μ_{eff} as the effective dipole moment of the charge-separated state surrounded by the solvent. In eq 4 it is assumed that the ground-state dipole moment is negligible, compared to that of the charge-separated state. If molecular rotation, described by the rotational time, τ_r, is fast, the polarization *P* can be treated as if at quasi-equilibrium and eq 1 can be rewritten

$$v + \tau_{RC}\frac{dv}{dt} = \Phi_{cs}\frac{RSV_0}{d}\frac{\varphi_c\mu_{cs}^2}{3k_BT}\frac{dn_{cs}}{dt} \tag{5}$$

where the quantum yield of formation of the charge-separated state, Φ_{cs}, scales the signal amplitude. Since the dipole moment is surrounded by a dielectric, instead of the effective dipole moment μ_{eff} we introduce a factor φ_c to account for the appropriate changes due to the dielectric. A simple approach for making this adjustment is to treat the problem in the semicontinuum Onsager model,[42] where a point dipole representing the dipole moment of a molecule is placed in the center of a spherical cavity of radius *a* (representing the molecule) and surrounded by a continuous dielectric with the dielectric constant of the solvent, ϵ. As a result of solvent polarization by the dipole, the reaction field from the solvent causes the dipole moment to increase due to its polarizability, α, and become

greater than its gas-phase value, μ_o[42]

$$\mu_{cs} = \frac{\mu_o}{1 - \frac{\alpha}{a^3}\frac{2(\epsilon - 1)}{2\epsilon + 1}} \quad (6)$$

The factor φ_c depends on the solvent dielectric constant, its refractive index, n_D, and the molecule's shape. For an ellipsoidal cavity it is given by[43]

$$\varphi_c = \left(\frac{\epsilon}{\epsilon + (\epsilon - 1)A_a}\right)^2 \frac{(2\epsilon + n_D^2)^2}{3(2\epsilon^2 + n_D^4)} \quad (7)$$

where the coefficient A_a refers to the case with the dipole moment oriented along the *a* semiaxis in the ellipsoid (the other two semiaxes being *b* and *c*) and is calculated from

$$A_a = \frac{abc}{2}\int_0^\infty \frac{ds}{(s + a^2)^{3/2}(s + b^2)^{1/2}(s + c^2)^{1/2}} \quad (8)$$

The coefficient simplifies to $A_a = 1/3$ for the case of a sphere. As shown before,[28,29] for spheroid the integral in eq 8 can be approximated using the aspect ratio, γ

$$A_a = \gamma/3 = b/3a \quad (9)$$

Alternatively,[43] for very elongated molecules such as triad **1**, A_a can be approximated as zero. Since, as we have shown,[29] the reaction field is much stronger than the external field, the dipole moment μ_{cs} in eq 6 can be interpreted as the dipole moment in that particular solvent.

The experiments were carried out in two modes.[29] The displacement current mode (load resistor, $R = 50\ \Omega$), where the *RC* time of the circuit is less than the lifetime of the charge-separated state, is almost free of adjustable parameters, and is most reliable for measuring dipole moments. The charge displacement mode ($R = 1\ M\Omega$) could only be used in solvents of low conductivity and is more suitable for measuring long charge-recombination times.

For systems such as **1** in MTHF or THF, where the charge-separated state decays exponentially with a time constant τ_{CR}, there are only three variable parameters for fitting the photoinduced voltage as a function of time to eqs 1−4: μ_{cs}, τ_r, and τ_{CR}. Each of these factors defines a unique feature in the signal.

Photoinduced Voltage Curves. Figure 3 shows the photoinduced voltage measured at ambient temperature in the displacement current mode for a THF solution of **1**. Excitation was with a 396 nm (Figure 3A) or 559 nm (Figure 3B) laser pulse. In both cases, the photoresponse has been normalized to an absorbed energy of 9.3 μJ. Each response consists of a positive region and a negative region of much smaller amplitude. The shape of the positive region is primarily a function of the rotation time, τ_r, and the initial dipole orientation defined by the polarization at excitation. To simplify, we excited at the magic angle but found almost no difference with other polarizations. That seems to be reasonable for this case, where transitions with two orthogonal polarizations in the porphyrin both result in the same charge-separated state and their combination produces close to uniform initial distribution of dipoles. The negative portion of the photoresponse reflects the lifetime of the charge-separated state, τ_{CR}. Since τ_{CR} is considerably longer than the laser pulse and molecular rotation portion of the signal, the amplitude of this negative portion is too small to permit one to obtain a precise value for the lifetime of $C^{\bullet+}-P-C_{60}^{\bullet-}$.

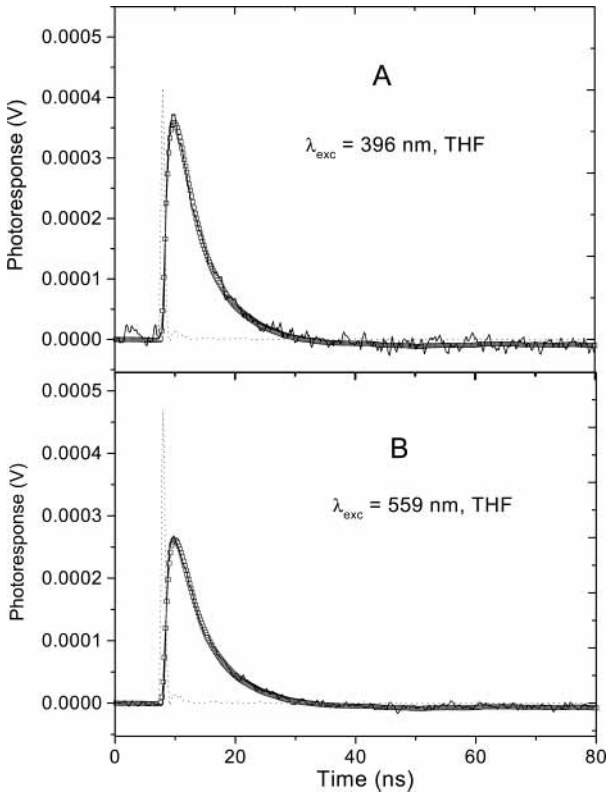

Figure 3. Solid lines are the photoresponse of $C-P-C_{60}$ triad **1** in tetrahydrofuran as measured in the displacement current mode in the cell with a 1.2 mm gap. Excitation was at 396 (A) or 559 (B) nm, and the responses have been normalized to the same amount of absorbed energy, 9.3 μJ. The squares represent the best fit to the experimental data and yield the parameter values reported in the text. The dotted lines show the shape of the laser excitation pulse.

Figure 4 shows the results of for **1** in 2-methyltetrahydrofuran taken under conditions similar to those used in Figure 3. Excitation was at 396 nm. The results in Figure 4A were obtained in the displacement current mode and are very similar to those obtained in tetrahydrofuran. The signal amplitude in the negative region is again too small to allow determination of a reliable charge recombination time. The data in Figure 4B were measured in the charge-displacement mode. In this mode, the rotational time τ_r is manifested in the rise time of the photoresponse, and the decay of the positive signal is a function of the lifetime of the charge-separated state, τ_{CR}.

Analysis of the Data. The results in Figures 3 and 4 were fitted by eqs 1−4 using methods previously described.[29] The results in tetrahydrofuran measured at either wavelength yield best fit rotational times τ_r of 7.5 ± 0.5 ns (the fits are shown in the figures). The corresponding data in Figure 4 give an indistinguishable value, 7.5 ± 0.5 ns. The similarity of these two times is expected, given the similar viscosities of the two solvents, but the time constants are somewhat high and require a detailed discussion, which we present later. The measurement in the charge-displacement mode (Figure 4B) allows determination of the lifetime of $C^{\bullet+}-P-C_{60}^{\bullet-}$ with an accuracy of ~10%: $\tau_{CR} = 300$ ns. This lifetime also yields reasonable fits to the decays of the small negative components of the displacement current curves in Figures 3 and 4A.

The amplitudes of the photoresponse curves in Figures 3 and 4 are related to the magnitude of the dipole moment of $C^{\bullet+}-P-C_{60}^{\bullet-}$. The magnitudes obtained by fitting to eqs 3 and 5 are insensitive to the factors governing τ_r mentioned above.[29] Without taking into account the less than unity quantum yield

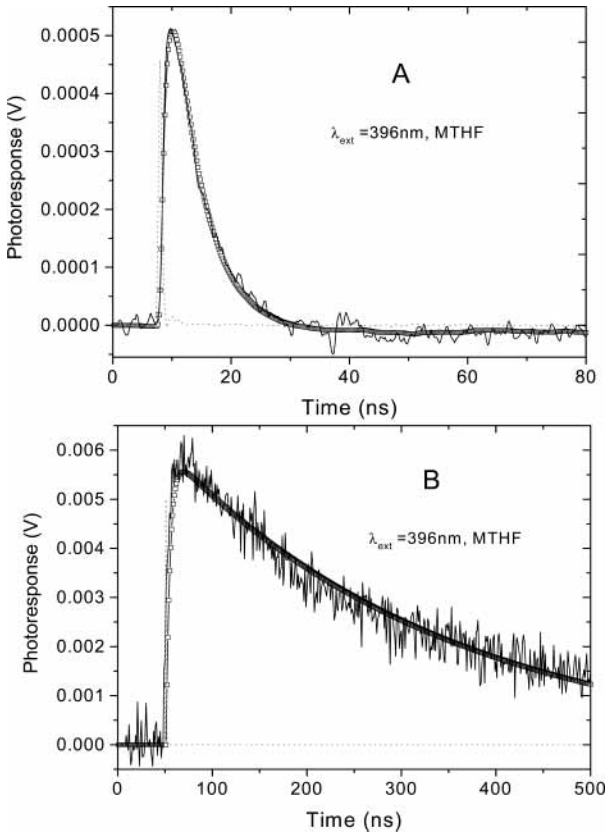

Figure 4. Solid lines are the photoresponse of C−P−C_{60} triad **1** in 2-methyltetrahydrofuran as measured in the cell with a 1.2 mm gap in the displacement current mode (A) and the charge displacement mode (B). Excitation was at 396 nm, and the responses have been normalized to the same amount of absorbed energy as in Figure 3, 9.3 μJ. The squares represent the best fit to the experimental data and yield the parameter values reported in the text. The dotted lines show the shape of the laser excitation pulse.

of charge separation (i.e., assuming $\Phi_{cs} = 1$) and taking $A_a \approx 0$[44] the fitting of the dipole signal in THF yielded μ_{cs} values of 109 D with excitation at 396 nm and 80 D, with 559 nm excitation. In MTHF with excitation at 396 nm, fitting the data from either the displacement current or charge displacement experiments under the abovementioned assumptions yielded $\mu_{cs} = 137 \pm 5$ D. The dielectric constants of tetrahydrofuran, ϵ-(THF) = 7.52 and 2-methyl-tetrahydrofuran, ϵ(MTHF) = 6.97 as well as their respective refractive indexes, n_D(THF) = 1.405 and n_D(MTHF) = 1.406, were taken from the literature.[45]

The apparent μ_{cs} values must be first corrected for the quantum yield Φ_{cs}. As mentioned above, the optically measured quantum yield of $C^{\bullet+}-P-C_{60}^{\bullet-}$ in THF is Φ_{cs} (THF) = 0.59. This yield is based on light absorbed only by the porphyrin or fullerene moieties. Light energy absorbed by the carotenoid is not transferred effectively (<10%) to the porphyrin in this molecule and is essentially ineffective in charge separation. The absorption spectrum of **1** is reasonably approximated by a linear combination of the spectra of porphyrin, carotenoid, and fullerene model compounds.[37] On this basis, at 396 nm, 91% of the absorption is due to the porphyrin and fullerene moieties. Thus, Φ_{396} (THF) = 0.91 × 0.59 = 0.54. With excitation at 559 nm, only 51% of the absorbed light is harvested by the porphyrin and fullerene moieties and Φ_{559} (THF) = 0.51 × 0.59 = 0.30. In MTHF, the yield of charge separation in **1**, at 0.88, is considerably higher than it is in tetrahydrofuran, and Φ_{396} (MTHF) = 0.91 × 0.88 = 0.80. When normalized by the yield, Φ_{cs}, the dipole moments in all three cases become identical within our accuracy, $\mu_{cs} = 153 \pm 6$ D. Note that if the spherical approximation for molecular shape were used in eq 7 (A_a = 1/3), the dipole moment would be considerably smaller, 110 D.

Discussion

Magnitude of the Dipole Moment. To the best of our knowledge, the dipole moment determined for $C^{\bullet+}-P-C_{60}^{\bullet-}$ surpasses previous champions[24−26,28] and is the largest ever experimentally determined for a single molecule. Division of the 153 D value by 4.8 D/Å yields a separation of 31.9 ± 1.2 Å between the centers of positive and negative charge. For comparison, the calculated conformation shown in Figure 1 suggests a separation distance of 34 Å between the center of negative charge placed at the center of fullerene and the center of positive charge in the center of carotenoid. The agreement is remarkable.

There are a few caveats to the above analysis. These include the possibilities of (i) oversimplification of molecular shape, (ii) Coulombic attraction between the polarizable chromophores, (iii) overestimation of the quantum yield of charge separation, and (iv) a conformational change in the charge separated state. Below we will discuss each possibility.

Molecular Shape. The approximation of $A_a = 0$ made above oversimplifies the effect of molecular shape. At the same time, for an extended molecule like triad **1**, approximation as an ellipsoid is also too far from reality. An alternative evaluation[43] is based on separating the contribution to the total dipole moment, M_{cs}, made by the solute, μ_{cs}, and the solvent polarized by the solute, M_s

$$M_{cs} = \mu_{cs} + M_s \tag{10}$$

This description is similar to that of Kirkwood's[46] but more simplified in our case. We enclose the solute in a spherical cavity of a larger radius and consider solvent inside as a continuum with the dielectric constant ϵ. Since triad **1** is much larger than the solvent molecules, such an approach is fairly accurate. For this "supermolecule", i.e., solute + solvent inside the cavity, one can use the Onsager approximation, i.e., neglect the interaction with other solvent. The contribution to the dipole moment from the solvent can be obtained by the integrating electric polarization, P, induced by the solute dipole. As suggested,[43] the latter can be found, without solving Poisson's equation, through a simplified approximation

$$\vec{M}_s = \int_{V \neq V_s} \vec{P}\, dV = \frac{\epsilon - 1}{4\pi\epsilon} \int_{V \neq V_s} \vec{E}_{vac}\, dV \tag{11}$$

where the electric field is approximated by the corresponding solution in a vacuum, E_{vac}, normalized by the solvent dielectric constant. Here the molecule's volume is excluded from the integration and the electric field in a vacuum E_{vac} is calculated from the charge distribution, $q_i(r_i)$, within the molecule

$$\vec{E}_{vac}(\vec{r}) = \sum_i \frac{q_i}{|\vec{r} - \vec{r}_i|^3} (\vec{r} - \vec{r}_i) \tag{12}$$

We apply this approach for calculating M_s and mimic the distribution of charges in the charge-separated state of triad **1** by placing a single negative unit charge in the center of the fullerene and distributing the positive charge evenly along the carotene backbone. The resulting value of the dipole moment M_s with that charge distribution is very weakly sensitive to the

van der Waals radii of the atoms, which are used to represent the molecular shape. Moreover, other distributions of positive charge with the same dipole moment, either with four-quarters of a unit charge on $C_{9'}$, $C_{13'}$, C_9, and C_{13} carbons or even just a single unit charge between C_{15} and $C_{15'}$ carbons, as labeled in Figure 1, provide the same result within 1% accuracy. Using van der Waals radii from the literature,[47] we calculated $M_s = -46 \pm 1$ D, which brings the total dipole moment of the charge transfer state to $\mu_{cs} = M_{cs} - M_s = 110 + 46 = 156 \pm 6$ D. That number is in better agreement with the expected value of 163 D = 34 Å × 4.8 D/Å calculated for the lowest energy conformation of the ground-state molecular structure shown in Figure 1.

Effect of Mutual Polarizability. Given the partial double-bond character of the amide bond linking the carotenoid and porphyrin moieties, the conjugated π-electron system of the carotenoid extends all the way to the point where the *meso*-aryl ring joins the porphyrin macrocycle. The orbital overlap is interrupted at this point because the steric influence of the flanking methyl groups forces the aryl ring nearly perpendicular to the macrocycle (Figure 1). It is therefore possible to write resonance structures for the carotenoid radical cation in which the positive charge resides close to the porphyrin macrocycle. Semiempirical AM1 calculations for β-carotene show that upon oxidation to the radical cation, charge is significantly delocalized over the 14 carbon atoms in the center of the π-electron system.[48] Thus, in the charge-separated state, Coulombic attraction by the negative charge on the fullerene would tend to move the center of positive charge on the carotenoid closer to the porphyrin, decreasing the dipole moment. If the polarizability of the carotenoid radical cation (and fullerene radical anion) were large enough, this effect would contribute to reducing the observed dipole moment. Semiempirical AM1 calculations on the radical cation of the carotenoid canthaxanthin show disappearance or significant lowering of the bond length alternation for the conjugated system, relative to the neutral carotenoid, and this would lead to an increase in electric polarizability.[49,50]

Krawczyk reported[50,51] experimental values for the transition moments of the first two optical absorptions of the radical cation of the carotenoid astaxanthin: $M_{01} = 7.5$ D ($E_{10} = 7810$ cm^{-1}) and $M_{02} = 16.$D ($E_{20} = 12000$ cm^{-1}). The ground-state polarizability α(carotene$^+$) of the cation radical can be estimated from these values using perturbation theory

$$\alpha = 2(M_{01}^2/E_{10} + M_{02}^2/E_{20} + ...) \approx 285 \text{ Å}^3 \qquad (13)$$

There are no experimental data on polarizability of fullerene anion radical. Semiempirical (AM1) calculations that we performed using HyperChem[38] suggest that it is close to that of a neutral molecule, $\alpha(C_{60}^-) = 80$ Å^3. Incidentally, analogous calculations for carotene$^+$ imply its anisotropic polarizability to be different from that of the neutral molecule, along the primary axis it is $\alpha_{||}$(carotene$^+$) ≈ 490 Å^3, while $\alpha_{||}$(carotene) ≈ 190 Å^3. The correction to the dipole moment due to the electric polarizability may be estimated[52] from eq 14

$$|\Delta\mu| = (\alpha(C_{60}^-) + \alpha(\text{carotene}^+))E \approx \alpha\frac{e}{\epsilon r^2} \qquad (14)$$

where r is the separation of the centers of positive and negative charge. Applying this equation to triad **1** and using the total polarizability $\alpha = 570$ Å^3 yields a correction of $\Delta\mu < 0.4$ D. The polarizability of the radical cation of the carotenoid moiety of **1** is likely somewhat higher than the above estimate, given further extension of the π-electron system in the dyad, but it still seems unlikely that the effect will contribute significantly.

Quantum Yield. Equation 5 indicates that overestimating the quantum yield of formation of $C^{\bullet+}-P-C_{60}^{\bullet-}$ will result in an underestimation of the dipole moment. Thus, this is in principle a possible cause for the slightly small measured dipole moment in **1**. The factors affecting the quantum yield measurement for **1** have been discussed.[37] The estimate is based on rate constants for the various electron-transfer and decay pathways for the relevant excited states in **1** and model compounds. Barring the occurrence of unexpected new decay pathways or unexpected changes in rate constants for the excited and intermediate charge-separated states in **1** relative to the model compounds, it is unlikely that the quantum yield estimates would be in error enough to account entirely for the differences between the observed and expected dipole moment. However, the occurrence of such unknown effects cannot be completely excluded as a possibility.

Molecular Conformation. If the molecular conformation of $C^{\bullet+}-P-C_{60}^{\bullet-}$ is different from that in Figure 1 and brings the centers of charge closer together, the measured dipole moment would be smaller than expected. There are a number of possibilities for such conformations, including rotation about the carbon−nitrogen amide bond of **1** to generate a cis conformation or generation of cis configurations or *s-cis* conformations in the carotenoid backbone. It is unlikely that any of these isomers are present to any appreciable extent in the ground state of the triad. X-ray and NMR data and MM+ calculations show the all-trans conformation in the amide and carotenoid backbone as the most stable.[39−41] However, it is conceivable that rotation about some bonds in the carotenoid chain may occur after formation of the radical cation to yield conformations with a smaller dipole moment. Semiempirical (AM1) calculations on β-carotene and similar carotenoids show that one-electron oxidation leads to significant bond length equalization between the single and double bonds in the entire conjugated carotenoid backbone between the β-ionyl rings.[48,49] This would be expected to facilitate rotation about bonds that are formally double in the ground-state structure. Indeed, Kispert and co-workers[49] reported that electrochemical or ferric chloride oxidation of all-trans canthaxanthin and β-carotene leads to significant trans to cis isomerization, with cis isomers occurring in about 40% of the products. The mechanism was proposed to be facile isomerization in the radical cation, followed by comproportionation reactions that regenerate neutral carotenoids. Calculations (AM1) of the transition-state energies for rotation about formally double bonds indicated much lower barriers for the radical cations than for the neutral species. The authors suggest that similar isomerizations could occur in carotenoid-containing molecules such as **1** that have long-lived charge-separated states.[49] If such carotenoid isomerization of the radical cation occurs in **1**, it could contribute to lowering the measured dipole moment.

Rotation Times. On the basis of simple hydrodynamic theory, the rotational diffusion time for a sphere of volume V in a medium of viscosity η is given by the Einstein law[53,54] as

$$\tau_{spher} = \frac{1}{6D} = \frac{V\eta}{k_B T} \qquad (15)$$

For a sphere with the van der Waals volume equal to that of triad **1**, $V = 1890$ Å^3, and for the solvent viscosity of THF, $\eta(25\ ^\circ\text{C}) = 0.46$ cP,[45] at room temperature ($T = 298$ K) one obtains the τ_{spher} value of 0.22 ns, which is over an order of magnitude smaller than the measured τ_r. As discussed above,

triad **1** is far from being a spherical molecule. Unfortunately, there is no a simple limiting approximation for rotation time for molecules with extended arbitrary shapes. The only approximation other than spherical is that of an ellipsoid of revolution, in which, according to Perrin,[55,56] there are two diffusion coefficients, $D_{||}$ and $D_{\perp}$, for rotation about the longitudinal and equatorial semiaxes

$$D_{||} = \frac{3(1 - \gamma S)}{2(1 - \gamma^2)} D \tag{16}$$

$$D_{\perp} = \frac{3\gamma[(2 - \gamma^2)S - \gamma]}{2(1 - \gamma^4)} D \tag{17}$$

Here the aspect ratio $\gamma = b/a$ has the same meaning as in eq 9, i.e., it is the ratio of the longitudinal and equatorial semiaxes. The value D is calculated from eq 15 for a sphere of the same volume. In the case of a prolate ellipsoid of revolution ($\gamma < 1$), S is given by

$$S = \frac{\gamma}{\sqrt{1 - \gamma^2}} [\ln(1 + \sqrt{1 - \gamma^2}) - \ln \gamma] \tag{18}$$

Approximating triad **1** as a prolate spheroid is still not a perfect representation of its shape—the definition of semiaxes is ambiguous. Nevertheless, if we use the van der Waals volume, V, and take the molecule's length to be the longitudinal axis, $2a \approx 55.2$ Å, we can estimate using eq 9 that $\gamma \approx 0.139$.[44] Equations 17 and 18 can be approximated in the limit of very small γ as[56]

$$\tau_{\perp} = \frac{1}{6D_{\perp}} \approx \frac{\tau_{\text{spher}}}{3\gamma^2(0.2 - \ln \gamma)} \tag{19}$$

where τ_{spher} is given by eq 15. For $\gamma \approx 0.139$, eq 19 gives the estimated rotational time about the equatorial semiaxis, $\tau_{\perp} = 1.8$ ns. This is closer to the measured value of 7.5 ns, but the applicability of eqs 16−19 for an extended molecule like triad **1** is very questionable. The calculated $\tau_{\perp}$ is very sensitive to many factors such as the aspect ratio γ and the charge distribution. For example, the value of $\tau_{\perp}$ will be increased up to the experimental value of $\tau_r \approx 7.5$ ns if one assumes a much smaller aspect ratio, $\gamma \approx 0.057$, while maintaining the same molecular volume. That aspect ratio corresponds to an "average" diameter of triad **1**, $2b \approx 3.2$ Å. Also, the hydrodynamic approximation underestimates the total friction for charge-transfer states. Triad **1** in its charge-transfer state produces a strong electric field over a large surrounding volume. The high amplitude of this field as well as its large gradient can noticeably alter solvent properties and the triad's interaction with the solute. As discussed in the literature, rotational relaxation of dipolar and ionic species in polar solvents can be slower than the hydrodynamic model suggests due to the so-called dielectric friction and solvent attachment effects.[57−59]

Lifetime of the Charge-Separated State. Between the two modes of dipole signal measurements, the most reliable determination of the decay characteristics of the giant dipole comes from the charge-displacement mode (Figure 4B), where the signal was found to decay exponentially with a time constant $\tau_{CR} \approx 300$ ns. Given the signal-to-noise ratio of the data in Figure 4B, this is consistent with the lifetime of 340 ns determined by transient absorption measurements in this solvent.[37]

Conclusions

The transient dc photocurrent measurements have verified the formation and decay of a giant dipole coincident with the light-induced formation and decay of the $C^{\bullet+}-P-C_{60}^{\bullet-}$ charge-separated state in triad **1**. The record magnitude of the dipole moment, ∼160 D, is close to the value estimated from the distance between the center of the negatively charged fullerene and a positive charge near the center of the carotenoid moiety for the molecule in an extended conformation, ∼33−34 Å. Given several conceivable sources of discrepancy in the treatment, this agreement is remarkable.

Experimental Section

Transient absorption measurements were made with excitation from an Opotek optical parametric oscillator pumped by the third harmonic of a Continuum Surelight Nd:YAG laser. The pulse width was ∼5 ns, and the repetition rate was 10 Hz. The detection portion of the spectrometer has been described elsewhere.[29]

Transient dc conductivity measurements were performed in a homemade transient displacement current cell[29] (see Figure 2). Excitation was by a Nd:YAG laser (Orion SB−R), and a TDS 684B digital oscilloscope (Tektronix) with a 1 GHz bandwidth was employed for signal detection. An external voltage of 500 V was applied across the cell's gap, either 1.2 or 0.7 mm. Two wavelengths were used: 396 (CH_4-shifted third harmonic) and 559 nm (CF_4-shifted second harmonic). The laser pulses were ca. 20 ps long and had less than 100 μJ of incident energy. All measurements were done at room temperature.

Acknowledgment. This work in part was supported by grants from the National Science Foundation (CHE-0078835), the Department of Energy (DE-FG02-86ER 13592), and the National Institute of Health (S06 GM 08136-26).

References and Notes

(1) Gust, D.; Moore, T. A. In *The Porphyrin Handbook*; Kadish, K. M., Smith, K. M., Guilard, R., Eds.; Academic Press: New York, 2000; Vol. 8, pp 153−190.

(2) Wasielewski, M. R. *Chem. Rev.* **1992**, *92*, 435−461.

(3) Gust, D.; Moore, T. A.; Moore, A. L. *Acc. Chem. Res.* **1993**, *26*, 198−205.

(4) Kurreck, H.; Huber, M. *Angew. Chem., Int. Ed. Engl.* **1995**, *34*, 849−866.

(5) Maruyama, K.; Osuka, A.; Mataga, N. *Pure Appl. Chem.* **1994**, *66*, 867−872.

(6) Sakata, Y.; Imahori, H.; Tsue, H.; Higashida, S.; Akiyama, T.; Yoshizawa, E.; Aoki, M.; Yamada, K.; Hagiwara, K.; Taniguchi, S.; Okada, T. *Pure Appl. Chem.* **1997**, *69*, 1951−1956.

(7) Gust, D.; Moore, T. A.; Moore, A. L. *Acc. Chem. Res.* **2001**, *34*, 40−48.

(8) Gust, D.; Moore, T. A.; Moore, A. L. *IEEE Eng. Med. Biol.* **1994**, *13*, 58−66.

(9) Ashton, P. R.; Johnston, M. R.; Stoddart, J. F.; Tolley, M. S.; Wheeler, J. W. *J. Chem. Soc., Chem. Commun.* **1992**, 1128−1131.

(10) Bissell, R. A.; de Silva, A. P.; Gunaratne, H. N.; Lynch, P. M.; Maguire, G. E.; Sandanayake, K. S. *Chem. Rev.* **1992**, *92*, 7−195.

(11) Debreczeny, M. P.; Svec, W. A.; Wasielewski, M. R. *Science* **1996**, *274*, 584−587.

(12) Gunter, M. J.; Johnston, M. R. *J. Chem. Soc., Chem. Commun.* **1992**, 1163−1165.

(13) Harriman, A.; Ziessel, R. *Chem. Commun.* **1996**, 1707−1716.

(14) Mirkin, C. A.; Ratner, M. A. *Annu. Rev. Phys. Chem.* **1992**, *43*, 719−754.

(15) O'Neil, M. P.; Niemczyk, M. P.; Svec, W. A.; Gosztola, D. J.; Gaines, G. L. I.; Wasielewski, M. R. *Science* **1992**, *257*, 63−65.

(16) Shiratori, H.; Ohno, T.; Nozaki, K.; Yamazaki, I.; Nishimura, Y.; Osuka, A. *Chem. Commun.* **1998**, 1539−1540.

(17) Wagner, R. W.; Lindsey, J. S.; Seth, J.; Palaniappan, V.; Bocian, D. F. *J. Am. Chem. Soc.* **1996**, *118*, 3996−3997.

(18) Chambron, J.-C.; Harriman, A.; Heitz, V.; Sauvage, J.-P. *J. Am. Chem. Soc.* **1993**, *115*, 7419−7425.

(19) Chambron, J.-C.; Harriman, A.; Heitz, V.; Sauvage, J.-P. *J. Am. Chem. Soc.* **1993**, *115*, 6109−6114.

(20) Linke, M.; Chambron, J.-C.; Heitz, V.; Sauvage, J.-P. *J. Am. Chem. Soc.* **1997**, *119*, 11329−11330.
(21) Warman, J. M.; de Haas, M. P. In *Time-Resolved Conductivity Techniques DC to Microwave, "Pulse Radiolysis"*; Tabata, Y., Ed.; CRC: Boca Raton, 1990; p 101.
(22) Fessenden, R. W.; Hitachi, A. *J. Phys. Chem.* **1987**, *91*, 3456.
(23) de Haas, M. P.; Warman, J. M. *Chem. Phys.* **1982**, *73*, 35.
(24) Paddon-Row, M. N.; Oliver, A. M.; Warman, J. M.; Smit, K. J.; de Haas, M. P.; Oevering, H.; Verhoeven, J. W. *J. Phys. Chem.* **1988**, *92*, 6958−6962.
(25) Warman, J. M.; de Haas, M. P.; Oevering, H.; Verhoeven, J. W.; Paddon-Row, M. N.; Oliver, A. M.; Hush, N. S. *Chem. Phys. Lett.* **1986**, *128*, 95−99.
(26) Warman, J. M.; de Haas, M. P.; Paddon-Row, M. N.; Cotsaris, E.; Hush, N. S.; Oevering, H.; Verhoeven, J. W. *Nature (London)* **1986**, *320*, 615−616.
(27) Visser, R. J.; Weisborn, P. S.; van Kan, P. J.; Huizer, B. H.; Varma, C. A. G. O.; Warman, J. M.; de Haas, M. P. *J. Chem. Soc., Faraday Trans. 2* **1985**, *81*, 689−1985.
(28) Smirnov, S. N.; Braun, C. L.; Greenfield, S. R.; Svec, W. A.; Wasielewski, M. R. *J. Phys. Chem.* **1996**, *100*, 12329−12336.
(29) Smirnov, S. N.; Braun, C. L. *Rev. Sci. Instrum.* **1998**, *69*, 2875−2887.
(30) Gust, D.; Mathis, P.; Moore, A. L.; Liddell, P. A.; Nemeth, G. A.; Lehman, W. R.; Moore, T. A.; Bensasson, R. V.; Land, E. J.; Chachaty, C. *Photochem. Photobiol.* **1983**, *37S*, 46.
(31) Moore, T. A.; Gust, D.; Mathis, P.; Mialocq, J.-C.; Chachaty, C.; Bensasson, R. V.; Land, E. J.; Doizi, D.; Liddell, P. A.; Lehman, W. R.; Nemeth, G. A.; Moore, A. L. *Nature (London)* **1984**, *307*, 630−632.
(32) Gust, D.; Moore, T. A. *Adv. Photochem.* **1991**, *16*, 1−65.
(33) Ohkouchi, M.; Takahashi, A.; Mataga, N.; Okada, T.; Osuka, A.; Yamada, H.; Maruyama, K. *J. Am. Chem. Soc.* **1993**, *115*, 12137−12143.
(34) Osuka, A.; Yamada, H.; Maruyama, K.; Mataga, N.; Asahi, T.; Yamazaki, I.; Nishimura, Y. *Chem. Phys. Lett.* **1991**, *181*, 419−426.
(35) Osuka, A.; Yamada, H.; Maruyama, K.; Mataga, N.; Asahi, T.; Ohkouchi, M.; Okada, T.; Yamazaki, I.; Nishimura, Y. *J. Am. Chem. Soc.* **1993**, *115*, 9439−9452.
(36) Osuka, A.; Yamada, H.; Shinoda, T.; Nozaki, K.; Ohno, O. *Chem. Phys. Lett.* **1995**, *238*, 37−41.
(37) Kuciauskas, D.; Liddell, P. A.; Lin, S.; Stone, S.; Moore, A. L.; Moore, T. A.; Gust, D. *J. Phys. Chem. B* **2000**, *104*, 4307−4321.
(38) HyperChem Release 6.0 Pro.; Hyprcube Inc.: Gainesville, FL.
(39) Chachaty, C.; Gust, D.; Moore, T. A.; Nemeth, G. A.; Liddell, P. A.; Moore, A. L. *Org. Magn. Reson.* **1984**, *22*, 39−46.
(40) Gust, D.; Moore, T. A.; Liddell, P. A.; Nemeth, G. A.; Makings, L. R.; Moore, A. L.; Barrett, D.; Pessiki, P. J.; Bensasson, R. V.; Rougée, M.; Chachaty, C.; de Schryver, F. C.; Van der Auweraer, M.; Holzwarth, A. R.; Connolly, J. S. *J. Am. Chem. Soc.* **1987**, *109*, 846−856.
(41) Gust, D.; Moore, T. A.; Moore, A. L.; Devadoss, C.; Liddell, P. A.; Hermant, R. M.; Nieman, R. A.; Demanche, L. J.; DeGraziano, J. M.; Gouni, I. *J. Am. Chem. Soc.* **1992**, *114*, 3590−3603.
(42) Onsager, L. *J. Am. Chem. Soc.* **1936**, *58*, 1486.
(43) Vlassiouk, I.; Smirnov S. *J. Phys. Chem. A* **2003**, 7561.
(44) We can take the molecule's length to be the longitudinal axis 2*a* and then calculate the equatorial axis 2*b* from the molecule's volume, $V = 4\pi ab^2/3$. Taking the molecule's total length to be the distance between the most remote atoms in the all trans conformation, $2a \approx 55.2$ Å, and the van der Waals volume from the modeling ($V = 1890$ Å^3), one calculates $b = 3.84$ Å, $\gamma \approx 0.139$ and $A_a \approx 0.046$.
(45) *Handbook of Organic Solvents*; Lide, D. R., Ed.; CRC Press: Boca Raton, FL, 1995.
(46) Kirkwood, J. *J. Chem. Phys.* **1939**, *7*, 911.
(47) Bondi, A. *J. Phys. Chem.* **1964**, *68*, 441.
(48) Broszeit, G.; Diepenbrock, F.; Gräf, O.; Hecht, D.; Heinze, J.; Martin, H.-D.; Mayer, B.; Schaper, K.; Smie, A.; Strehblow, H.-H. *Liebigs Ann. Chem.* **1997**, 2205−2213.
(49) Gao, G.; Wei, C. C.; Jeevarajan, A. S.; Kispert, L. D. *J. Phys. Chem.* **1996**, *100*, 5362−5366.
(50) Krawczyk, S. *Chem. Phys.* **1998**, *230*, 297−304.
(51) Krawczyk, S. *Chem. Phys. Lett.* **1998**, *294*, 351−356.
(52) Mylon, S. E.; Smirnov, S. N.; Braun, C. L. *J. Phys. Chem.* **1998**, *102*, 6558−6564.
(53) Einstein, A. *Ann. Phys.* **1906**, *19*, 371−371.
(54) Fleming, G. R.; Morris, J. M.; Robinson, G. W. *Chem. Phys.* **1976**, *17*, 91−100.
(55) Perrin, F. *J. Phys. Radium* **1934**, *5*, 497−511.
(56) Perrin, F. *J. Phys. Radium* **1936**, *7*, 1−11.
(57) Spears, K. G.; Steinmettz, K. M. *J. Phys. Chem.* **1985**, *89*, 3623−3629.
(58) Horng, M.-L.; Gardecki, J. A.; Maroncelli, M. *J. Phys. Chem. A* **1997**, *101*, 1030−1047.
(59) Kumar, P. V.; Maroncelli, M. *J. Chem. Phys.* **2000**, *112*, 5370−5381.